International Journal of Design & Nature and Ecodynamics
Vol. 20, No. 11, November, 2025, pp. 2493-2505
Journal homepage: http://iieta.org/journals/ijdne

Comparative Study on Performance, Combustion, and Emissions of a Diesel Engine Fueled with Various Biodiesels and Blends

Abdelkader Bendriss[1*], Hamza Bousbaa[2], Cheikh Kezrane[3], Khaled Loubar[4], Yahia Lasbet[3]

[1] Department of Mechanical Engineering, RESA Laboratory, University Ziane Achour of Djelfa, Djelfa 3117, Algeria
[2] Department of Mechanical Engineering, LTE Laboratory, National Polytechnic School Maurice Audin, Oran 1523, Algeria
[3] Department of Mechanical Engineering, LDMM Laboratory, University Ziane Achour of Djelfa, Djelfa 3117, Algeria
[4] Energy Systems and Environment Department, GEPEA Laboratory, IMT Atlantique, Nantes 44307, France

Corresponding Author Email: a.bendriss@univ-djelfa.dz

https://doi.org/10.18280/ijdne.201102

Received: 27 October 2025
Revised: 22 November 2025
Accepted: 27 November 2025
Available online: 30 November 2025

Keywords:
biodiesels, physicochemical properties, combustion, performance, emissions, statistical analysis

ABSTRACT

The use of fossil fuels has caused environmental pollution and contributed to global warming. Biodiesel is a biofuel with similar physicochemical properties to those of diesel and can be produced from a variety of raw materials. In this study, a thermodynamic modeling of combustion in a Lister-Petter-TS1 diesel engine was conducted, based on experimental measurements of the pressure-signal in the combustion chamber, to understand the influence of physicochemical properties on the combustion process. The engine was powered by seven different fuels: standard diesel and 6 types of biodiesels based on waste cooking oils (WCO), animal fat residues (AFR), palm oils (PO), and blends of 10%, 20%, and 30% of biodiesel from olive mill wastewater. The experiments were conducted at an engine speed of 1500 rpm and under different loads (25%, 50%, 75%, and 100%). The results showed that the six tested biofuels give performances comparable to those of diesel, with a significant reduction in pollutant emissions. Biodiesels showed an increase in specific fuel consumption (5%). Using B100-WCO showed a lower emission level for particulate matter (50%), unburned hydrocarbons (62%), with the exception of NOx, which recorded a slight increase of (3%). Statistical analysis shows a good agreement between the obtained results.

1. INTRODUCTION

The limitation in the availability of petroleum-based fuels and environmental concerns have created the need to find alternative fuel sources such as biofuels, wind energy, solar energy, hydroelectric energy, hydrogen, nuclear energy, and so on [1]. Among all these alternative energy sources, biofuels are one of the potential alternative energy sources that can meet some of the current energy demand [2]. The concept of biofuels dates back to the 19th century when researchers tried to use vegetable oil as fuel for diesel engines. Due to the rapid depletion of petroleum-based fuels and the increasing consumption of fuels in developing countries, and environmental concerns, researchers and governments are developing renewable energy-based fuels [3, 4].

Biofuels are fuels obtained from renewable and non-fossil materials. The synthesis of gaseous fuels can be done from plant or animal biomass (di-hydrogen or methane) or charcoal, alcohol can be obtained by fermentation of hydrolyzed starch or sugars, and biodiesel from vegetable oil or animal fat [5, 6]. We also distinguish first-generation biofuels, originating from agro-resources for food purposes, and second-generation biofuels, from lignocellulosic sources (leaves, wood, straw, etc.), third-generation biofuels (Algo-fuels), from micro-algae [7, 8]. Depending on their nature, biofuels can be found in liquid or gaseous state, used mainly for the transport sector, they can be used alone or in mixtures with a conventional fuel [9]. One of the advantages of these alternative fuels is their use in existing engines without modifications or with minimal modifications [10]. However, various processes (thermochemical or biochemical) can be used to obtain these alternative fuels [11]. Consequently, their compositions are different, and their physicochemical properties can vary from one fuel to another [12]. This induces variations in engine performance in terms of thermal efficiency, specific consumption, and especially pollutant emissions [13].

Biodiesel is a biofuel that has similar properties to conventional diesel [14]. In addition, it is renewable and emits fewer polluting emissions compared to petroleum diesel when burned. Like all fuels, it has its advantages and disadvantages. Its first advantage is that it can be used in direct injection engines as a pure fuel or in blends with conventional diesel [15].

Biodiesel is technically defined as a fuel consisting of a mixture of fatty acid esters derived from vegetable oils or animal fats. Theoretically, any vegetable oil or animal fat that comprises predominantly saturated or unsaturated long-chain fatty acid triglycerides can be used in diesel engines [16, 17]. However, early research using crude vegetable oils as fuel in diesel engines resulted in various engine problems, such as

atomization problems, injector fouling, sticking, carbon deposits on the piston and cylinder head of the engine, excessive engine wear, and contamination of the lubricating oil during prolonged operation [18, 19]. These problems are commonly attributed to the physicochemical properties of vegetable oils and/or animal fats. Therefore, it has been recommended by many researchers to use thermochemical or hydrothermal liquefaction processes to reduce the high viscosity of vegetable oils or animal fats. Transesterification is a widely used process that allows the conversion of vegetable oils and animal fats into biodiesel so that they can be used in diesel engines [20]. After liquefaction, the viscosity of biodiesel became between 7 and 11 times lower than that of the parent oil, which improves the atomization and volatility of the air-fuel mixture and makes combustion more complete [21]. In addition, the higher viscosity of biodiesel than that of conventional diesel gives it better lubricity in the combustion chamber (CC), which reduces friction and wear of mechanical parts. The high flash point makes handling biodiesel safer. The higher cetane number of biodiesel than that of diesel makes it ignite more quickly [22, 23].

The recovery of these used oils into biodiesel prevents their discharge into the sewerage network and therefore protects water treatment facilities and the environment. Many researchers have reported that the production of biodiesel from waste cooking oils (WCO), animal fat residues (AFR), palm oils (PO), and olive mill wastewater (OMWW) is more profitable than that of virgin oils. The cost of producing biodiesel from WCO is 2.5 to 3.0 times cheaper than that of virgin vegetable oils, which could significantly reduce the total production cost of biodiesel and make it competitive with conventional diesel [24, 25].

Many researchers have established the suitability of WCO biodiesel; despite this, these studies report a wide disparity in the results obtained, especially regarding emission levels [10]. A construction of combustion, performance, and emission characteristic maps can provide appropriate insights to explain the discrepancy reported in the literature [13]. Compared with conventional diesel fuel, biodiesel has many advantages, such as biodegradability, low toxicity, low particulate and CO emissions, high flash point (> 130°C), low sulfur and aromatic content, and inherent lubrication ability [26]. Nevertheless, it has been noted that used cooking oil may exhibit some negative effects, such as the formation of acid polymers and glycerols. These effects lead to an increase in the viscosity of the used oil and an increase in free fatty acid contents [27]. Furthermore, the presence of high water content in WCO leads to a reduction in biodiesel yield during transesterification by the competing saponification reaction.

Although several studies have been conducted on the combustion of several biodiesels in compression ignition engines, little data are available on the performance of an engine fueled by biodiesels from animal fat residues (AFR) [28]. Moreover, the study of AFR ethanol emulsions on diesel engines seems to have been carried out by a few researchers. Animal fats had the advantage of mixing freely with alcohols (methanol or ethanol), and these blends can be used in existing diesel engines without modification [29]. The main advantages of the blend are the absence of technical modifications and the ease of implementation. Blending animal fats with alcohols results in a significant improvement in physicochemical properties [30], viscosity and density are considerably reduced, and volatility is also improved.

Olive oil can be used to produce biodiesel through a chemical transesterification process, which involves mixing the oil with an alcohol, such as methanol or ethanol, in the presence of a catalyst (NaOH or KOH) to create a mixture of esters, which is biodiesel. The resulting biodiesel is chemically similar to conventional diesel and is produced in significant quantities from the triglycerides present in olive oil. Olive oil extraction generates some negative environmental effects, such as water pollution. The generated olive mill wastewater (OMWW) varies between 0.3 and 1.1 m^3 per ton of processed olives, depending on the extraction process used. Different processes are used for the conversion of OMWW into different types of chemical products, such as gasification, pyrolysis, and combustion [9]. Among the most suitable conversion techniques for biofuel production is hydrothermal liquefaction (HTL). It is the most practical because it does not require upstream drying of the biomass [9].

In this work, a modeling of combustion in a compression ignition engine, fueled by 7 fuels, namely standard diesel and 6 types of biodiesels based on (waste cooking oils; animal fat residues; palm oils; and blends of B10, B20, and B30 of biodiesel from olive mill wastewater), is carried out. The thermodynamic model of combustion was programmed, with the use of experimental measurements recorded in the IMT Atlantique laboratories of Nantes, France, carried out on a test bench equipped with a Lister-Petter TS1 engine. These measurements were carried out at different engine loads. The pressure signal provided by the test bench is a signal that includes noise, to be smoothed (filtered). The Savitzky-Golay method is used, this for a good understanding of the engine responses in terms of combustion.

The objective of this article is, therefore, firstly, to test the influence of the physicochemical properties (kinematic viscosity, density, cetane number, low heating value) of the analyzed fuels on engine responses in terms of combustion, performance, and pollutant emissions. Secondly, to analyze statistically the correlations between the tested loads and the resulting engine responses. The aim is to identify the relationships between the tested engine loads in terms of combustion characteristics, performance, and pollutant emissions.

2. MATERIALS AND METHODS

2.1 Measuring equipment

Figure 1 shows a detailed diagram of the entire test bench, as well as the acquisition means used. This test bench is mainly composed of a diesel engine (Lister Petter TS1 series), a dynamometric brake, an exhaust gas analysis bay, a particle analyzer, and a fuel supply system.

An electric dynamometer is used to drive and load the engine. A differential pressure transmitter of the LPX5841 type ensures the measurement of the flow rate and the intake air temperature. This sensor is linked to a buffer capacity, ensuring the attenuation of pressure waves upstream of the sensor. A Coriolis flow meter of the RHM015 type linked to a transmitter of the RHE08 type measures the mass flow rate of fuel consumed by the engine. The test bench is also equipped with a system of type K thermocouples, which ensures the measurement of the various temperatures (exhaust temperature, fuel temperature, etc.). The ambient temperature is measured using a temperature and humidity sensor of the HD 2012 TC/150 type.

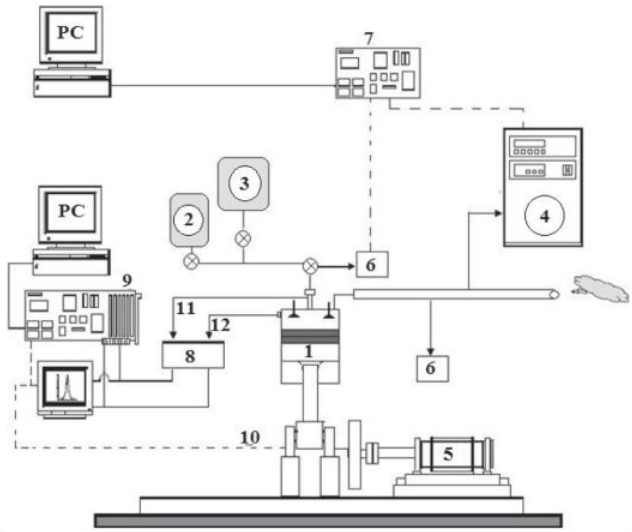

(1) Test Engine, (2) Biofuel Tank, (3) Diesel Fuel Tank, (4) Exhaust Gas Analyzer, (5) Eddy Current Dynamometer, (6) Particulate Matter Analyzer, (7) Low Frequency Data Acquisition System, (8) Charge Amplifier, (9) High Frequency Data Acquisition System, (10) Crank Angle Encoder/ Speed Sensor, (11) Injection Pressure Signal, (12) Cylinder Pressure Signal

Figure 1. Schematic diagram of the test engine setup

The test bench is equipped with an acquisition system equipped with an AVL 364C angular encoder that measures the angular position of the crankshaft as well as the engine speed. This encoder can achieve an accuracy of 0.1 crankshaft angle degrees (°CA). A water-cooled piezoelectric sensor (AVL QH32D), which is introduced into the combustion chamber at the cylinder head, ensures the measurement of the cyclic pressure in the cylinder. A PMP 4070 absolute pressure transmitter located in the intake manifold measures the intake pressure. A piezoelectric sensor of the AVL QH33D type measures the fuel injection pressure; it is positioned in the hose connecting the injection pump to the injector. The channel of a pollutant emissions analysis bay is linked to the exhaust pipe. The fraction of exhaust gases passing through the analysis bay will be dehydrated before being analyzed. The pollutants measured in this bay are unburned hydrocarbons by FID flame ionization using a GRAPHITE 52M hydrocarbon analyzer. Nitrogen oxides (NO and NOx) are measured by chemiluminescence using a TOPAZE 32M nitrogen oxide analyzer. Carbon monoxide, dioxide, and oxygen (CO, CO_2, and O_2) are measured using a MIR 2M infrared detector.

In this study, cylinder pressure measurements were recorded every 100 consecutive cycles, with sampling intervals of 0.1, 0.2, and 0.5 crankshaft angle degrees (°CA). Before each test, the engine was calibrated according to the manufacturer's catalog values. All data were collected after the engine had stabilized. Throughout the tests, the operating parameters of the test engine were fixed as follows: injection timing of 13°CA before top dead center (TDC), engine speed of 1500 rpm, and compression ratio of 18.

2.2 Analysis methods

The analysis model used to calculate the heat release is based on the first law of thermodynamics. The heat release of the engine cycle is calculated by the method initially proposed by Krieger and Borman [31]. Assuming that the combustion chamber contains a homogeneous mixture of ideal gases having reached thermodynamic equilibrium. Applying the law of conservation of energy to the closed part of the cycle during the period when the valves are closed (i.e., between the closing of the intake valve and the opening of the exhaust valve), gives the following expression:

$$dQ_{comb} = m.C_v.dT + P.dV + dQ_p + \frac{dm_f}{d\theta} h_f \qquad (1)$$

With Q_{comb} is the heat released by combustion, h_f is the enthalpy of gases, Q_p is the heat lost through the cylinder walls.

According to Heywood [32], the amount of combustion heat from gas leaks does not exceed 2% of the amount of fuel injected. Neglecting these leaks and applying the ideal gas law to the previous equation (Eq. (1)), we obtain:

$$\frac{dQ_{comb}}{d\theta} = \frac{C_v}{r} V.\frac{dp}{d\theta} + (\frac{C_v}{r} + 1)P.\frac{dV}{d\theta} + \frac{dQ_P}{d\theta} \qquad (2)$$

Discretizing this equation using a simple Euler scheme gives a system of algebraic equations to be solved systematically over intervals of 0.1, 0.2, and 0.5°CA of the crankshaft. This gives the profile of the instantaneous overall heat release rate by fuel combustion and the profile of the cumulative heat release. The heat lost through the cylinder walls is given by:

$$\begin{cases} \sum \frac{dQ_{paroi}}{d\theta} = \sum \frac{dQ_{paroi}}{dt} \frac{dt}{d\theta} \\ \sum \frac{dQ_{paroi}}{dt} = h_c.A.(T - T_w) \\ \frac{dt}{d\theta} = \frac{1}{6N} \end{cases} \qquad (3)$$

where, h_c is the convection heat transfer coefficient, A is the surface area of the cylinder walls, N is the engine rotation speed, T and T_w are the gas temperature and the wall temperature, respectively. The wall temperature is estimated at 340.15K [32], while the combustion chamber temperature is calculated according to the first principle of thermodynamics. To calculate Q_p, several approaches are used; in our study, we used the Woshnie correlation since it gives good results in terms of thermal convection [10].

Heat release analysis can provide very important information about the combustion process, which helps to explain the evolution of the maximum cycle pressure, the formation of pollutants and the engine efficiency.

3. RESULTS AND DISCUSSIONS

Once the biodiesel is produced and deemed acceptable, it must be used as fuel in diesel engines. Tests are carried out on the engine test bench at IMT Nantes. This test bench is equipped with a Lister Petter single-cylinder four-stroke diesel engine (Figure 1), whose characteristics are shown in Table 1.

To test the influence of physicochemical properties on the combustion of biodiesel in an ICE, a thermodynamic model calculation code is written, and seven fuels are tested. These fuels are subdivided into standard diesel and six biodiesels extracted from WCO, PO, AFR, and three blends from olive

mill wastewater (B10, B20, and B30 from OMWW). The properties of the six biodiesels, as well as standard diesel, are density, kinematic viscosity, low heating value (LHV), cetane number (CN), and flash point (FP), shown in Table 2.

Table 1. Lister Petter engine specification

Lister Petter–TS 1 Series	
General information	4 strokes, natural aspiration
Number of cylinders	1
Cooling system	Air cooled
Stroke	88.94 mm
Bore	95.5 mm
Connecting rod length	165.3 mm
Volumetric ratio	18:1
Maximum power	4.5 kW at 1500 rpm
Swept volume	630 cc
Injection timing	13°CA before TDC
Injection pressure	250 bar

Table 2. Properties of diesel fuel, biodiesel, and their blends

Fuels	Kinematic Viscosity (mm^2/s)	Density (kg/m^3)	LHV (MJ/kg)	CN	FP (°C)
B0-Diesel	2.3	800	43.45	51	59.85
B100-WCO	4	860	38,152	56.1	159.85
B10-OMWW	1.9	832.79	42.91	57.88	77
B20-OMWW	2.22	838.75	42.46	56.12	74
B30-OMWW	2.58	846.75	41.87	56.63	73
B100-AFR	5.13	870	40	53	
B100-PO	11.1	900	40.5	54	

3.1 Combustion analysis

In order to analyze the combustion characteristics, it is necessary to monitor the evolution of the pressure signal in the cylinder because the measurement of this pressure provides the necessary information to interpret the combustion process. For this, it is essential to analyze the phenomena that occur in the combustion chamber from fuel injection to the end of combustion. Engine tests are carried out at a constant engine speed of 1500 rpm for four engine loads 25%, 50%, 75%, and 100%. Cylinder pressure and injection pressure measurements are taken every 0.5°CA for B100 of palm oil; 0.1°CA for B100 of animal fat residues; and 0.2°CA for other biodiesels and standard diesel.

3.1.1 Cylindrical pressure

The evolution of the cylindrical pressure as a function of the crankshaft angle allows us to describe the course of combustion during an engine cycle and to estimate the start of combustion to deduce which fuel burns better than the other.

Figure 2 shows the peak cylinder pressures as a function of four engine loads for the tested fuels. It can be seen that, under the same engine load conditions, the peak cylinder pressures of biodiesels and their blends are comparable to those of diesel fuel. As the engine load increases, the maximum cylinder pressure increases, and pressure peaks occur further from the TDC, which avoids the knocking problem of the engine.

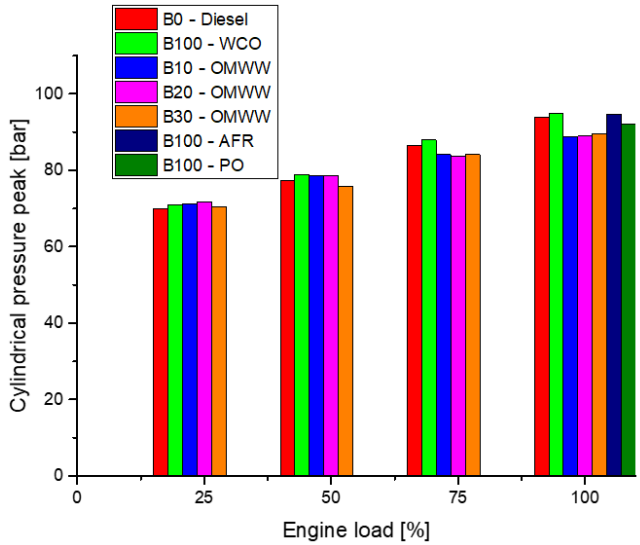

Figure 2. Pressure peaks as a function of engine load

Table 3. Summary statistics of peak pressure

Variable	Observations	Minimum	Maximum	Mean	Std. Deviation
25%	5	69.963	71.691	70.871	0.670
50%	5	75.791	78.994	77.876	1.359
75%	5	83.775	87.898	85.253	1.821
100%	7	88.818	95.031	91.862	2.728

At 25% engine load, the peak pressure values are almost the same for the tested fuels, with a standard deviation of 0.67 bar. It is noted that the pressure standard deviation between engine loads begins to widen with increasing engine load (Table 3). The maximum standard deviation of 2.728 bar is recorded at full engine load, but it is not very large. The cylinder pressure is almost the same for the tested fuels at each engine load.

For biodiesel, the presence of oxygen in its chemical composition promotes combustion. Furthermore, the cetane number (CN) of biodiesel (53-57.88) is higher than that of diesel (51), resulting in faster combustion and therefore a shorter ignition delay [26]. However, the kinematic viscosity of biodiesel is greater than that of diesel (Table 2), which leads to poor atomization of the air-fuel mixture, resulting in a delayed start of combustion. In fact, ignition delay is strongly negatively correlated with CN; that is, if the fuel CN increases, ignition delay decreases [26]. However, a slight advance towards TDC of the peak pressure of biodiesel compared to diesel for all loads is observed, which can cause an engine-knocking problem; this therefore affects the durability of the engine. Fortunately, this advance is always before TDC. In the present study, the peak remains at 3.8°CA degrees away from TDC.

3.1.2 Cylindrical temperature

The combustion temperature provides information about

combustion efficiency. The peak temperature depends on the fraction of fuel burned during the initial combustion phase. Figure 3 presents the peak temperatures at all tested engine loads for the seven fuels. From Figure 3, it is noticed that at 25% engine load, the peak temperatures are almost the same; the highest value is recorded for B0-diesel of 1429.4 K, while the lowest value is for B30-OMWW of 1383.7 K, with a standard deviation of 16.457 K (Table 4). For 50 and 75% of engine load, the gap starts to widen by 49.013 and 67.104 K, respectively. At full engine load, the peak temperature values are 1915.3, 1884.1, 2047.8, 1900.6, 1879.9, 2123.6, and 1975.4 K, respectively, for B0-diesel; B100-WCO, B10-OMWW; B20-OMWW; B30-OMWW; B100-AFR, and B100-PO (Figure 3). It is observed that the difference in temperature peaks becomes significant by 93.459 K. Furthermore, B100-WCO and B30-OMWW recorded almost the same peak temperature.

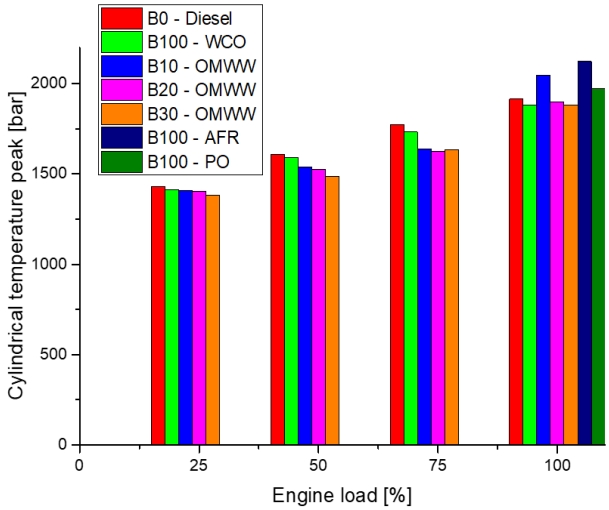

Figure 3. Temperature peaks as a function of engine load

Table 4. Summary statistics of peaks temperature

Variable	Observations	Minimum	Maximum	Mean	Std. Deviation
25%	5	1383.700	1429.400	1407.280	16.457
50%	5	1489.000	1609.500	1551.160	49.013
75%	5	1627.500	1774.100	1682.060	67.104
100%	7	1879.900	2123.600	1960.957	93.459

At lower engine loads, the combustion chamber (CC) wall and residual gas temperatures decrease, resulting in a lower temperature at the time of injection; therefore, the ignition delay increases [10]. In general, the maximum combustion temperature for biodiesel is lower than that of conventional diesel. Except for full engine load, B100 gave the highest values. For medium and low loads, the calorific value of biodiesel is lower than that of conventional diesel. The CC temperature depends on the combustion rate, which in turn is influenced by the amount of fuel present in the premixed combustion phase, this phase governed by the ignition delay (ID). For high engine loads, the high viscosity and lower volatility of biodiesels lead to poor atomization and poor preparation of the mixture with air. The latter generates a significant mass of fuel injected into the CC, with the existence of oxygen in the chemical composition of biodiesel, which gives a higher temperature peak for B100 than the other fuels tested.

3.1.3 Heat release rate

Heat release rate (HRR) analysis is very important to analyze the combustion operation, in which we can extract the ignition delay, combustion duration (CD), energy released by the system, etc. To analyze the different phases of the combustion operation easily, filtering the cylinder pressure signal is essential, on which the calculation of the energy released by the system depends.

The pressure signal given by the test bench is a signal that includes noise; to filter it, the Savitzky-Golay (SG) method is used. The SG smoothing filter is considered a type of finite impulse response (FIR) digital filtering, represented by polynomial equations. Based on the least squares method, the SG filter is generally used to smooth a noisy signal whose frequency range of the noise-free signal is large. In this type of application, the SG filter performs better than standard FIR filters, as these tend to attenuate a significant portion of the high frequencies of the signal with noise.

Although the SG filter is more effective at preserving relevant high-frequency components, SG filters are less effective at removing high-level noise in a signal. The particular formulation of the SG filter preserves higher-order moments much better than other methods. As a result, the peak widths and amplitudes for desired signals tend to be preserved.

In the present study, a third-degree polynomial is used with 21 points for waste cooking oils and blends of olive mill wastewater, 51 points for animal fat residues, and 5 points for palm oils. The variation of the points supported by the polynomial is due to the measurement step of the pressure signal (0.2°CA for B100-WCO, B10-OMWW, B20-OMWW, B30-OMWW; 0.1°CA for B100 AFR; and 0.5°CA for B100-PO).

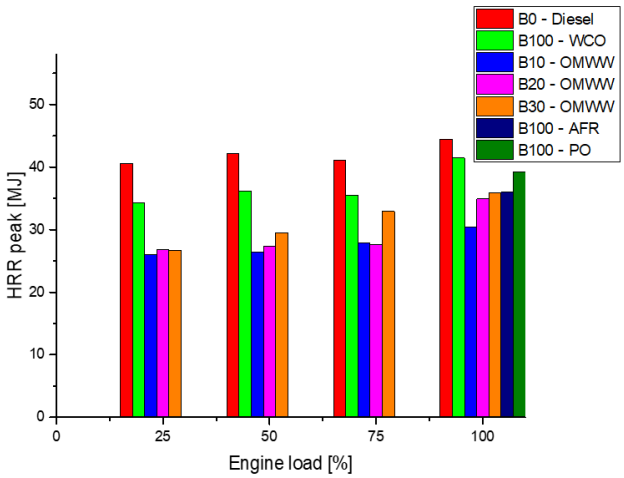

Figure 4. Heat release rate as a function of engine load

By applying the SG smoothing (filtering) method for a 3rd degree polynomial. It is found that the cylindrical pressure curves for all the fuels studied are almost identical; the difference is observed in the calculation of the cylinder

pressure derivative as well as for the heat release rate.

Figure 4 presents a comparison between the seven tested fuels according to the loads studied. It is noticed that diesel recorded the highest values of HRR peaks for all loads. While B10 from OMWW recorded the lowest values of HRR peaks (Table 5). It is also noticed that B100 gave higher peaks than OMWW blends. In addition, it was noticed that HRR peaks increase with the increase in engine load.

Table 5. Summary statistics of HRR

Variable	Observations	Minimum	Maximum	Mean	Std. Deviation
25%	5	25.953	40.548	30.815	6.406
50%	5	26.335	42.181	32.300	6.721
75%	5	27.644	41.042	32.993	5.600
100%	7	30.339	44.484	37.475	4.655

A certain amount of energy is required for the vaporization of the injected fuel, so a downward slope of TDC can be seen during the ignition delay. Biodiesel, due to its high cetane number, gives a shorter ignition delay compared to petroleum diesel. After the ignition delay, it can be seen that biodiesels and their blends start combustion earlier than petroleum-diesel, which takes longer to ignite, which leads to more fuel being injected before the start of combustion, which leads to a greater amount of fuel accumulation in the combustion chamber at the time of the premixed combustion phase. This leads to the explanation that the peak of heat release rate for petroleum-diesel is higher due to greater volatility and better mixing of diesel with air.

Table 6. Correlation matrix between engine load and HRR

Variables	25%	50%	75%	100%
25%	**1**			
50%	0.989	**1**		
75%	0.931	0.972	**1**	
100%	0.912	0.941	0.912	**1**

Table 6 presents a descriptive statistical analysis to extract the correlations between the studied loads and the tested fuels. It can be seen that strong positive correlations, Pearson coefficient > 0.91 (91%), are recorded for all loads. From these results, we can conclude that all loads carry the same information. Therefore, to analyze the evolution of HRR, it is enough to test a load and estimate the engine behavior for any other loads that we want to study.

The heat release rate depends mainly on fuel properties such as cetane number, LHV, and the fuel's ability to mix well with air. The peak of HRR depends on the combustion rate in the initial stage, which in turn is influenced by the amount of fuel burned in the first phase of combustion (the premixed phase).

3.1.4 Ignition delay

The ignition delay (ID) is the time that elapses between the start of fuel injection and the start of combustion. This parameter is important to correctly analyze the combustion process and to give further explanations on the behavior of both the cylinder pressure and the heat release rate. According to the literature, the ID is composed of two periods. The first is the physical delay period (PDP), and the second is the chemical delay period (CDP). The PDP period is related to the mixing of air with the atomization, vaporization, and decomposition of the fuel, as reported by Heywood [32]. Regarding the CDP, it represents the time required for the combustion initiation reaction.

Figure 5 shows the variation of ignition delay as a function of engine load for the analyzed fuels. The ID decreases with increasing engine load (engine power) for all the studied fuels. This can be explained by the increase in cylinder temperature and pressure, as well as the equivalence ratio of the air-fuel mixture. In addition, standard diesel gave a longer ID compared to biodiesel and its blends. From Figure 5, it can also be seen that B100 biodiesels gave the smallest ID. This is due to the high cetane number of biodiesel compared to standard diesel.

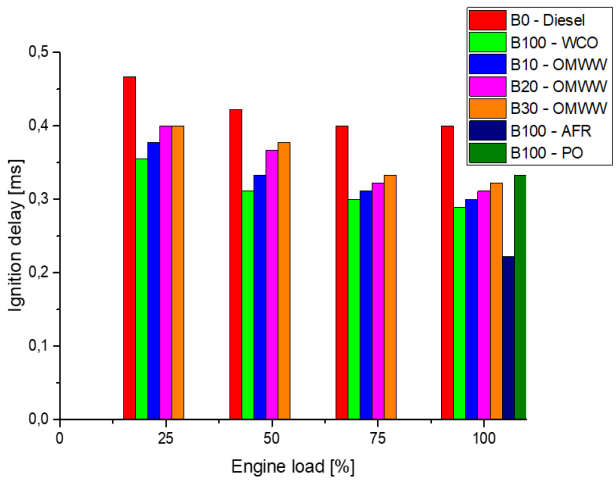

Figure 5. Ignition delay as a function of engine load

Table 7. Summary statistics of ID

Variable	Observations	Minimum	Maximum	Mean	Std. Deviation
25%	5	0.356	0.467	0.400	0.042
50%	5	0.311	0.422	0.362	0.043
75%	5	0.300	0.400	0.333	0.039
100%	7	0.222	0.400	0.311	0.053

From Figure 5, the ignition delay of biodiesels and their blends is shorter than that of standard diesel, since the onset of combustion of biofuels is faster compared to diesel (Table 7). This is due to the high cetane number of biodiesel compared to standard diesel, and the presence of oxygen in the molecules (chemical composition) of biodiesel, which helps in the

production of free oxygen radicals that promote the vaporization of the air-fuel mixture. In addition, it can be seen that, for all the loads studied, the ignition delay of pure biodiesels was shorter than that of the other fuels tested. This result can be explained by the increase in the gas temperature in the cylinder that promotes auto-ignition, which reduces the ID.

Table 8. Correlation matrix between engine load and ID

Variables	25%	50%	75%	100%
25%	**1**			
50%	0.973	**1**		
75%	0.983	0.937	**1**	
100%	0.978	0.925	0.999	**1**

Table 8 presents the correlation matrix between engine loads and the tested fuels. It can be observed that at all engine loads, there is a strong positive correlation, with a Pearson coefficient > 0.92 (92%). Therefore, to investigate the evolution of fuel IDs as a function of engine load. It is sufficient to test them at one load and estimate the rest.

3.1.5 Combustion duration (CD)

The CD is the period that elapses between the beginning of combustion (auto-ignition point) and the end of combustion. In the literature, there are several methods to determine the angle corresponding to the beginning and the end of combustion, either by analyzing the signal of the derivative of the pressure in the cylinder, or by analyzing the signal of the heat release rate [10]. The combustion operation can be explained as a sequence of chemical reactions; the duration of each reaction respects the typical phenomenology of combustion in a compression ignition engine (diesel engine). The combustion operation is subdivided into three phases. It begins with a premix combustion phase characterized by a rapid advancement of the reaction, followed by a diffusion phase in which the period of this phase is controlled by the injection of fuel, and finally a late phase that completes the combustion operation [29].

Figure 6 shows the evolution of combustion duration as a function of engine load. It can be seen that biodiesels and their blends have a longer combustion duration compared to petroleum diesel. In addition, the combustion duration of each fuel analyzed increases with increasing engine load for all tested loads. In addition, the standard deviation between the fuels is less; the largest deviation value is recorded at full engine load of the order of 0.107 ms (Table 9). It can be said that biodiesels and their blends give a better combustion duration than standard diesel.

Table 10 presents the correlation matrix between the tested loads as a function of the combustion duration of the analyzed fuels. A strong positive correlation is recorded between 25% and 50% loads, as well as for 75% and 100% loads. On the other hand, weak correlations are recorded between low loads and full loads.

The blends from olive mill wastewater recorded longer combustion duration than standard diesel and even pure biodiesel. This is due to the high LHV close to diesel, and the lower kinematic viscosity, which promotes atomization and vaporization of the air-fuel mixture. This leads to better combustion. Since the lower heating value of diesel is higher than that of biodiesels and their blends, this generates a higher quantity of fuel injected to maintain the same effective power as diesel; the quantity of fuel injected into the cylinder is greater, and it takes a longer time to burn. On the other hand, the presence of oxygen in the chemical (molecular) composition of biofuel promotes combustion.

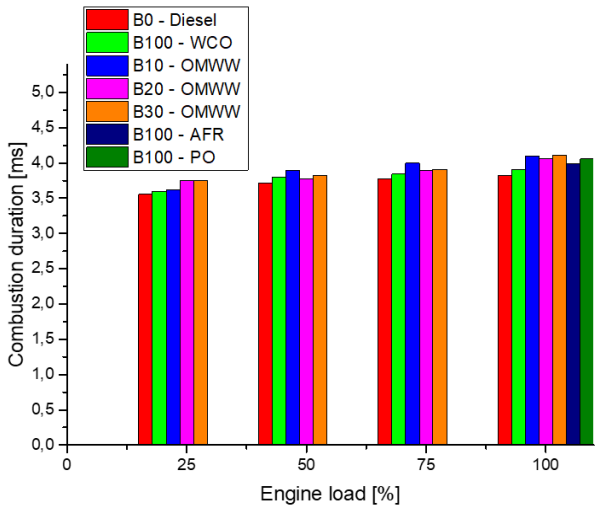

Figure 6. Combustion duration as a function of engine load

Table 9. Summary statistics of CD

Variable	Observations	Minimum	Maximum	Mean	Std. Deviation
25%	5	3.556	3.756	3.658	0.092
50%	5	3.711	3.889	3.800	0.065
75%	5	3.778	4.000	3.884	0.082
100%	7	3.822	4.111	4.008	0.107

Table 10. Correlation matrix between engine load and CD

Variables	25%	50%	75%	100%
25%	**1**			
50%	0.974	**1**		
75%	0.592	0.538	**1**	
100%	0.519	0.457	0.995	**1**

3.2 Engine performance

3.2.1 Brake specific fuel consumption

The brake specific fuel consumption (BSFC) of an engine is, by definition, equal to the ratio between the hourly mass flow rates of the fuel consumed and the effective power developed by the engine. The BSFC measures the efficiency with which an engine uses the injected fuel to produce work [26]. It thus allows two engines, which may have different cylinder capacities, to be compared. It is generally expressed in g/kWh.

From Figure 7, as engine power increases, BSFC decreases for all fuels analyzed. Standard diesel recorded the lowest BSFC, while the highest BSFC was recorded for B30 from OMWW. The standard deviation between the BSFC of the tested fuels is significant, especially for B100, and it starts to decrease with increasing load (see Table 11). It can be noted that the BSFC of B100 (WCO, AFR, and PO) is slightly higher compared to diesel. This is mainly due to the lower heating value of B100, which requires an increase in fuel consumption

to maintain the same effective engine power as diesel. In addition, a higher cetane number with lower viscosity of B10 from OMWW contributes to lower BSFC compared to B20 and B30 from OMWW. At full load, B100 from palm oils recorded the lowest brake specific consumption, close to standard diesel; this is due to the high LHV and density of this fuel.

Table 12 shows the correlations between engine loads and BSFC. It can be seen that strong positive correlations are recorded for all loads. It can be said that all loads carry the same information. Therefore, to test BSFC, it is sufficient to test one load and estimate the remaining loads.

Table 11. Summary statistics of BSFC

Variable	Observations	Minimum	Maximum	Mean	Std. Deviation
25%	5	374.000	480.000	419.400	44.719
50%	5	281.000	352.000	312.200	28.926
75%	5	260.000	318.000	284.400	22.601
100%	7	252.000	314.000	279.143	22.184

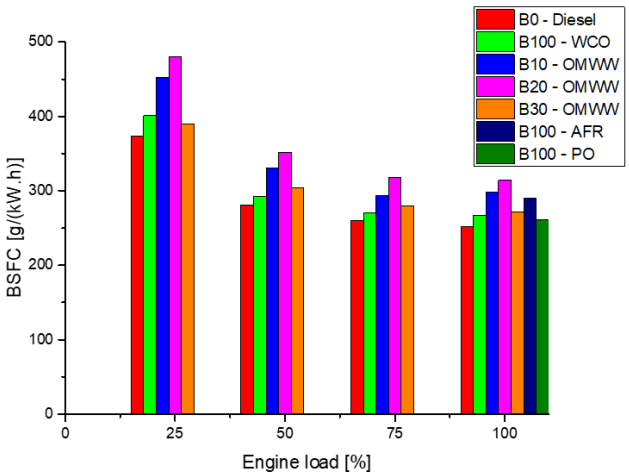

Figure 7. BSFC as a function of engine load

Table 12. Correlation matrix between engine load and BSFC

Variables	25%	50%	75%	100%
25%	**1**			
50%	0.973	**1**		
75%	0.953	0.991	**1**	
100%	0.983	0.997	0.984	**1**

3.2.2 Brake thermal efficiency

In thermal machines, the thermal energy supplied by the fuel is not fully converted into mechanical energy. The engine efficiency or brake thermal efficiency (BTE) considers this reality and includes all energy losses, both thermal and mechanical. To this end, the effective efficiency of an engine is the ratio of the effective power collected on the shaft to the thermal power supplied by the fuel.

Figure 8 shows the evolution of the brake thermal efficiency (BTE) as a function of the engine load. It is noted that the efficiency increases with increasing engine load for all the fuels analyzed. Biodiesel from waste cooking oils showed comparable performances to petroleum-diesel, with a slight increase in the BTE. In addition, blends from OMWW recorded the lowest values of BTE.

It is noted that the BTE is simply the inverse of the product of the brake specific fuel consumption (BSFC) and the low heating value of the fuel [26]. This leads to an increase in the brake specific fuel consumption for biodiesel, to compensate for the lower heating value of biodiesels and their blends. From Table 13, the B100 from WCO recorded the maximum brake thermal efficiency for all the loads tested. Whereas, the B30 from OMWW recorded the minimum BTE.

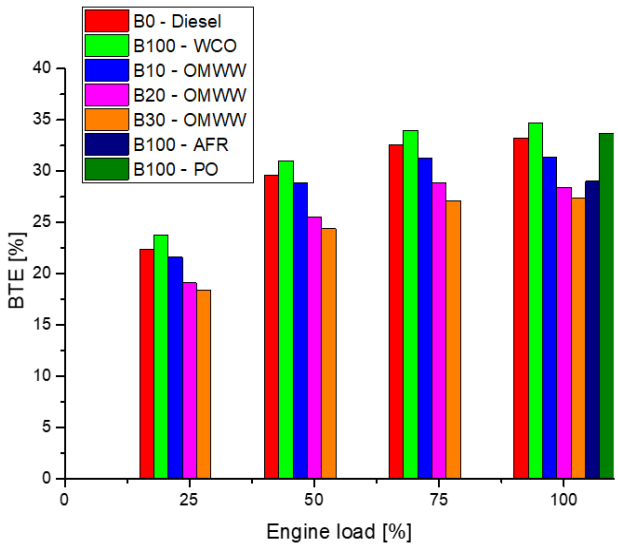

Figure 8. BTE as a function of engine load

From Table 14, we can see that there are very strong positive correlations of the order of > 99% between all the loads analyzed according to the brake thermal efficiency. That is, each load carries the same information as the other. Therefore, to analyze the influence of the engine load on the effective efficiency, it is enough to test it at one load and estimate its behavior on the remaining loads.

Table 13. Summary statistics of BTE

Variable	Observations	Minimum	Maximum	Mean	Std. Deviation
25%	5	18.400	23.800	21.060	2.265
50%	5	24.400	31.000	27.880	2.807
75%	5	27.100	34.000	30.780	2.785
100%	7	27.400	34.700	31.114	2.875

Table 14. Correlation matrix between engine load and BTE

Variables	25%	50%	75%	100%
25%	**1**			
50%	0.996	**1**		
75%	0.992	0.991	**1**	
100%	0.997	0.990	0.992	**1**

3.3 Polluting emissions

3.3.1 Nitrogen oxides

Nitrogen oxides (NOx) are formed when combustion reaches very high temperatures. In fact, there are two conflicting explanations for the formation of nitrogen oxides (NOx), but both link their formation to combustion chamber temperature. The first, less common, explanation attributes the higher NOx levels in biodiesel compared to conventional diesel to the high viscosity of biodiesel, which leads to poor atomization of the air-fuel mixture, resulting in incomplete combustion and a higher combustion chamber temperature. The second, more common, explanation attributes the higher NOx levels in biodiesel to the presence of oxygen in its chemical structure. This results in a short ignition delay (ID) and a long combustion duration (CD), ensuring efficient combustion of the air-fuel mixture, and consequently, a higher combustion chamber temperature [26]. These conditions are achieved during the combustion of a mixture close to stoichiometry in a high-pressure and temperature environment. According to Heywood [32], the maximum temperature range of the cycle is the most contributing to the formation of nitrogen oxides, that is, after the start of combustion and near the maximum pressure of the cycle. In this range, NOx is formed until reaching a maximum, then the temperature begins to decrease, and the NOx decomposes for a certain time before stabilizing until the exhaust.

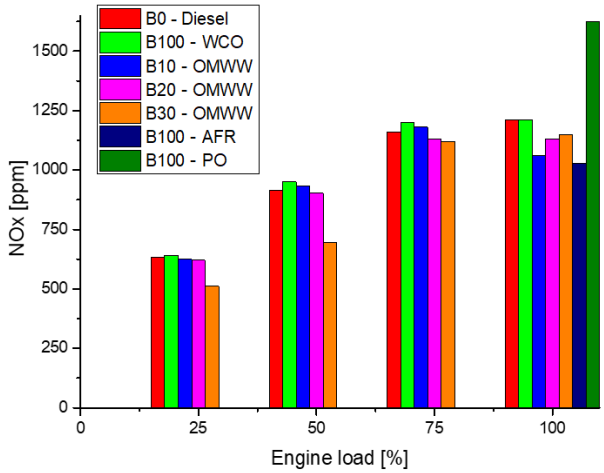

Figure 9. Concentration evolution of NOx in the exhaust gases

Table 15. Summary statistics of Nox

Variable	Observations	Minimum	Maximum	Mean	Std. Deviation
25%	5	511.000	640.000	605.600	53.454
50%	5	694.000	950.000	879.400	105.161
75%	5	1120.000	1200.000	1158.000	33.466
100%	7	1028.000	1625.830	1201.976	199.202

Figure 9 presents the NOx emission concentration in the exhaust gases at different engine loads for all fuels analyzed. It can be seen that the NOx emission concentration increases with increasing engine load and reaches its maximum level at full load. This is mainly due to the high combustion temperature influenced by the accumulation of injected fuel quantities. In addition, B100 from WCO recorded the highest NOx concentration, while at full load, B100 from palm oils recorded the highest value, due to their higher kinematic viscosity (11.1 mm²/s). B30 from OMWW has the lowest NOx emission concentration for all loads, except at full load, B100 from AFR has the lowest NOx emission concentration.

Table 16. Correlation matrix between engine load and NOx

Variables	25%	50%	75%	100%
25%	**1**			
50%	0.992	**1**		
75%	0.712	0.755	**1**	
100%	0.132	0.040	0.146	**1**

From Table 15, it was found that the standard deviation between NOx concentrations starts to increase with increasing engine load. At full load, B100 from palm oils recorded the highest value of 1625.83 of NOx emissions. From Table 16, it can be noticed that there is a strong positive correlation of 99.2% of NOx concentration between 25% and 50% loads, and lesser correlations are recorded for the rest of the loads (see Table 16). Several factors, such as high combustion temperature, oxygen content, and residence time in the high temperature zone, can increase NOx production. By inspecting the C/H and C/O ratios of different fuels, B30 from OMWW has the lowest value. This lower combustion stoichiometry leads to lower cycle temperature and reduces NOx formation when using B30 from OMWW.

3.3.2 Carbon monoxide (CO)

CO is an intermediate combustion product that will subsequently be oxidized to CO_2. Its formation is primarily related to the richness of the mixture of air and fuel and evolves in a manner similar to the formation of PM particles.

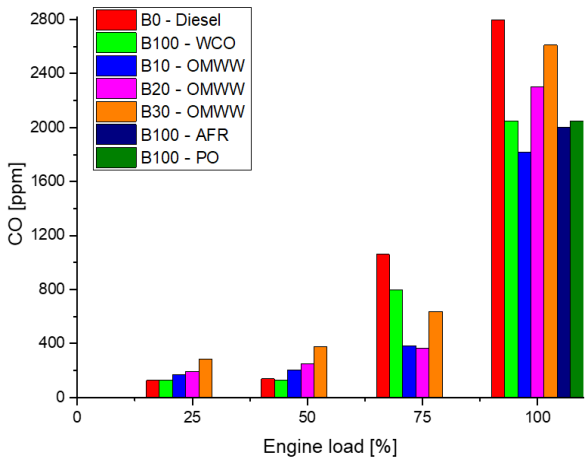

Figure 10. Evolution of CO concentration in exhaust gases

The variation of carbon monoxide (CO) emissions with engine load when the engine is running on the seven fuels is given in Figure 10. At 25% and 50% load, the fuels show similar emission rates, with only a small increase recorded for B30 from OMWW. As engine power increases, the amounts of CO emitted from the exhaust begin to differ between the fuels, and the standard deviation increases (Table 17). Biodiesel gives noticeably lower CO levels compared to diesel. This may be due to the oxygen content in the chemical composition of biodiesel and the higher combustion temperature, which encourages the oxidation of CO to CO_2. A strong positive correlation of 99.7% is recorded between the 25 and 50% load, while for the other loads, weak correlations are recorded. The carbon monoxide emissions for diesel at full engine load are 2800 ppm, and for B10-OMWW, they have been reduced by 1820 ppm.

Table 17. Summary statistics of CO

Variable	Observations	Minimum	Maximum	Mean	Std. Deviation
25%	5	126.100	285.000	179.540	65.522
50%	5	128.500	379.000	220.620	102.055
75%	5	365.000	1060.200	648.080	292.274
100%	7	1820.000	2800.000	2232.857	355.889

Table 18. Summary statistics of UHC

Variable	Observations	Minimum	Maximum	Mean	Std. Deviation
25%	5	65.780	267.000	211.216	83.715
50%	5	70.760	271.000	220.532	84.672
75%	5	89.330	312.000	253.286	93.097
100%	7	120.000	512.000	327.086	119.603

At low engine loads, the fuel mixture is lean, meaning that the mixture contains a significant amount of oxygen to oxidize the CO into CO_2. However, at high loads, the engine requires a significant amount of fuel, with the air flow unchanged, and the mixture becomes rich. There is, therefore, less oxygen available, which explains the sharp increase in carbon monoxide emissions. Indeed, the poor atomization of the fuel results in mixtures that are rich in some places and lean in others, so this mixture will burn poorly, resulting in incomplete combustion and high CO emissions.

3.3.3 Unburned hydrocarbons

Unburned hydrocarbons (UHC) are one of the important parameters for describing the emission behavior in a diesel engine. The UHC emissions are mainly related to the combustion process. Because if a hydrocarbon mixture does not encounter enough oxygen at a high enough temperature to complete combustion, it will be emitted with the exhaust gases.

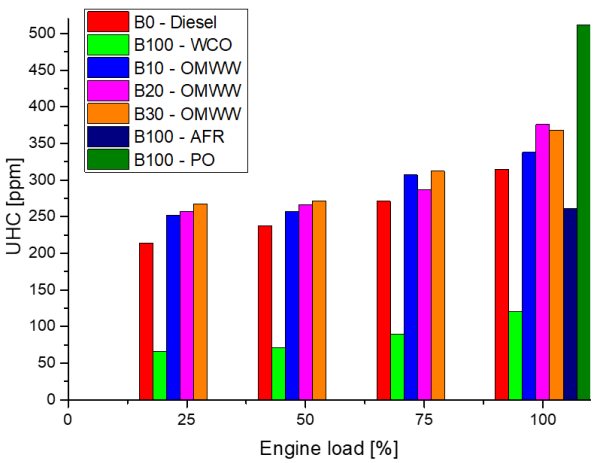

Figure 11. Evolution of UHC in exhaust gases

The variation of UHC emissions as a function of engine load is illustrated in Figure 11. It is found that B100 from WCO emits significantly lower UHC emissions compared to diesel fuel and other fuels tested. This is mainly due to the presence of oxygen in the chemical composition of B100-WCO, which improves the combustion quality inside the combustion chamber, resulting in more complete combustion. While the blends from OMWW have high values of UHC emissions. Indeed, during the diffusive combustion phase, the oxygen present in the molecular composition of biodiesel makes the zone fuel-rich, which increases the concentration of UHC in the exhaust gas. On the other hand, the high cetane number of pure biodiesel reduces the ignition delay, which has a significant effect on the reduction of UHC emissions. At full load (effective power of 4.5 kW), B100 from palm oil reported the highest UHC emissions, which may be due to the high viscosity of this fuel, which leads to poor atomization of the air-fuel mixture, resulting in incomplete combustion of this fuel.

Table 19. Correlation matrix between engine load and UHC

Variables	25%	50%	75%	100%
25%	**1**			
50%	0.995	**1**		
75%	0.992	0.993	**1**	
100%	0.993	0.995	0.978	**1**

Table 18 represents a descriptive analysis of the evolution of the concentration of unburned hydrocarbons (UHC) in the exhaust gases when using different fuels at the four loads analyzed. The UHC emissions increase with increasing engine load, as does their standard deviation. It can be seen that operation with pure biodiesel (B100) emits lower hydrocarbon levels compared to all other fuels, with the exception of B100 from PO. The presence of very rich fuel zones leads to incomplete combustion, and the fuel, instead of being burned, will be decomposed into hydrocarbons of more or less long chains. If these hydrocarbon molecules do not reach enough oxygen at a temperature sufficient to complete their combustion, they will be released with the engine exhaust gases. Table 19 presents the correlation matrix between the loads according to the concentration of unburned hydrocarbons. It is noted that there are strong positive

correlations with a Pearson coefficient > 0.97.

3.3.4 Particulate matter

Particulate matter (PM) is part of the exhaust gases of a diesel engine. It can be seen in the form of smoke or soot emissions.

During combustion, some injected fuel droplets burn partially or incompletely at a high combustion chamber temperature, so they are emitted in the form of carbon particles. The conversion of fuel into carbon particles is likely to occur when the engine is operating at high speed and high load, as can be clearly seen in Figure 12. In this case, the amount of injected fuel increases, leading to higher levels of smoke emissions. In addition, fuel-rich locations, where there is not enough oxygen, can significantly increase the amount of carbon particles or smoke emissions.

From Figure 12, it can be seen that the highest PM values are recorded for B30 from OMWW at low and medium loads. While diesel recorded the highest value at full load. On the other hand, pure biodiesel also reported the lowest PM emissions. Furthermore, B10 and B20 from OMWW have almost identical PM emissions as diesel at low load; the gap widens at full load. From Table 20, it can be seen that the standard deviation of PM emissions increases almost fivefold with the increase in load from 4.24 mg/m^3 at low load to 25.345 mg/m^3 at full load. We notice that there are strong positive correlations between low and medium loads, with a Pearson coefficient greater than 0.93. While at full load, weak correlations are recorded.

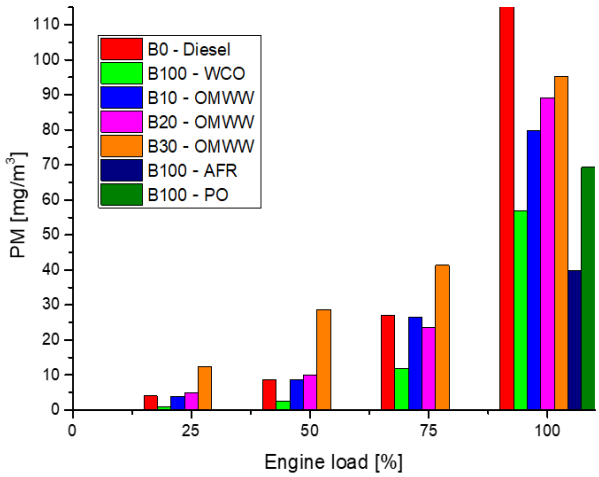

Figure 12. Evolution of PM concentration in exhaust gases

Table 20. Summary statistics of PM

Variable	Observations	Minimum	Maximum	Mean	Std. Deviation
25%	5	0.900	12.300	5.226	4.240
50%	5	2.500	28.700	11.660	9.950
75%	5	11.800	41.300	26.020	10.526
100%	7	39.700	116.000	78.000	25.345

The presence of oxygen in biofuel, in addition to that contained in the intake air, improves the mixing process, which leads to preparing more fuel for the premixing combustion phase. The higher cetane number of biofuel produces early combustion. In addition, the duration of this combustion phase is slightly shorter for conventional diesel. All the reasons mentioned above lead to reducing PM in the exhaust for biodiesel. For conventional diesel, the ignition delay with more fuel injected in the premixing phase increases PM emissions.

4. CONCLUSIONS

To model biodiesel combustion in an internal combustion engine, seven fuels were tested. Waste cooking oils, palm oils, animal fat residues, B10, B20, and B30 blends from olive mill wastewater, and standard diesel were the fuels analyzed in terms of combustion, performance, and pollutant emissions. Due to the variety of raw materials used for the production of these fuels, engine responses varied from one fuel to another. To this end, a statistical analysis was conducted to analyze the influence of biodiesels on engine loads in terms of combustion, performance, and pollutant emissions.

Analysis of combustion results shows that all analyzed fuels exhibit similar heat release rates (HRR). Biodiesel and its blends have a lower calorific value (38.153 to 42.91 MJ/kg) than standard diesel fuel (43.45 MJ/kg), so an additional quantity of fuel was injected to compensate for this energy difference. Furthermore, the density of biodiesel (832.79 to 900 kg/m^3) is higher than that of standard diesel fuel (800 kg/m^3), and since the injection pump is a volumetric pump, the mass of the injected biodiesel is greater than that of diesel fuel. This explains the slightly higher specific consumption of biodiesel (BSFC) compared to diesel fuel.

Pure biodiesel fuels exhibited the shortest ignition delay (ID), while blends of OMWW fuels had longer combustion duration (CD). This is due to the higher cetane number (CN) of biodiesel and its blends (53-57.88) compared to diesel (51), resulting in a shorter ID for biodiesel. Furthermore, the oxygen content of biodiesel fuels promotes combustion of the air-fuel mixture, contributing to their longer CD compared to diesel.

The OMWW blends recorded the lowest NOx emissions and higher HC emissions, while the highest NOx emissions were recorded for diesel, due to the high combustion chamber temperature. The B10-OMWW blend recorded the lowest CO emissions, due to its lower kinematic viscosity (1.9 mm^2/s), resulting in good air-fuel mixture atomization and therefore efficient combustion, influenced by the oxidation of CO to CO_2.

The analysis results show a strong correlation between engine response and load. These results were statistically analyzed to extract the correlations between loads and engine responses for the seven fuels analyzed. Based on the analysis of the seven fuels, it can be concluded that B20-OMWW fuel achieved the best results in terms of combustion, performance, and pollutant emissions.

REFERENCES

[1] Hoekman, S.K., Broch, A., Robbins, C., Ceniceros, E., Natarajan, M. (2012). Review of biodiesel composition, properties, and specifications. Renewable and

Sustainable Energy Reviews, 16(1): 143-169. https://doi.org/10.1016/j.rser.2011.07.143
[2] Ambaye, T.G., Vaccari, M., Bonilla-Petriciolet, A., Prasad, S., Hullebusch, E.D., Rtimi, S. (2021). Emerging technologies for biofuel production: A critical review on recent progress, challenges and perspectives. Journal of Environmental Management, 290: 112627. https://doi.org/10.1016/j.jenvman.2021.112627
[3] Algayyim, S.J.M, Yusaf, T., Naseer, H., Wandel, A.P., Fattah, M.R., Laimon, M., Rahman, S.M. (2022). Sugarcane biomass as a source of biofuel for internal combustion engines (ethanol and acetone-butanol-ethanol): A review of economic challenges. Energies, 15(22): 8644. https://doi.org/10.3390/en15228644
[4] Fitri, N., Khofifah, Royhan, H., Prakoso, N.I., Firdaus, F., Sukri, Q., Setiapraja, H. (2025). Essential oils and their fractions as biodiesel additives: A review on quality and performance enhancement. International Journal of Design & Nature and Ecodynamics, 20(8): 1847-1864. https://doi.org/10.18280/ijdne.200815
[5] Ravikumar, R., Hashmi, M.A., Shankar Ganesh, L., Bikkannavar, S.V., Vivek, D.R. (2019). Biofuel production and characterization from waste chicken skin and pig fat. International Journal of Recent Technology and Engineering, 8(3): 3598-3603. https://doi.org/10.35940/ijrte.C5312.098319
[6] Hasan, M., Abedin, M.Z., Amin, M.B., Nekmahmud, Md., Oláh, J. (2023). Sustainable biofuel economy: A mapping through bibliometric research. Journal of Environmental Management, 336: 117644. https://doi.org/10.1016/j.jenvman.2023.117644
[7] Kumar, S., Jain, S., Kumar, H. (2020). Experimental study on biodiesel production parameter optimization of jatropha–Algae oil mixtures and performance and emission analysis of a diesel engine coupled with a generator fueled with diesel/biodiesel blends. ACS Omega, 5(28): 17033-17041. https://doi.org/10.1021/acsomega.9b04372
[8] Satputaley, S.S., Zodpe, D.B., Deshpande, N.V. (2016). Performance, combustion and emission study on CI engine using microalgae oil and microalgae oil methyl esters. Journal of the Energy Institute, 90(4): 513-521. https://doi.org/10.1016/j.joei.2016.05.011
[9] Hadhoum, L., Zohra Aklouche, F., Loubar, K., Tazerout, M. (2021). Experimental investigation of performance, emission and combustion characteristics of olive mill wastewater biofuel blends fuelled CI engine. Fuel, 291: 120199. https://doi.org/10.1016/j.fuel.2021.120199
[10] Bendriss, A., Kezrane, C., Lasbet, Y., Awad, S., Loubar, K., Makhlouf, M. (2017). Experimental investigation on the influence of a biodiesel (waste cooking oil) on the performance and exhaust emissions of a compression ignition engine. Journal Européen des Systèmes Automatisés, 50(4-6): 361-378. https://doi.org/10.3166/JESA.50.361-378
[11] Nogueira, R.C., Neto, F.S., de Sousa Junior, P.G., Valério, R.B.R., et al. (2023). Research trends and perspectives on hydrothermal gasification in producing biofuels. Energy Nexus, 10: 100199. https://doi.org/10.1016/j.nexus.2023.100199
[12] Giakoumis, E.G. (2013). A statistical investigation of biodiesel physical and chemical properties, and their correlation with the degree of unsaturation. Renewable Energy, 50: 858-878. https://doi.org/10.1016/j.renene.2012.07.040
[13] Cheikh, K., Sary, A., Khaled, L., Abdelkrim, L., Mohand, T. (2016). Experimental assessment of performance and emissions maps for biodiesel fueled compression ignition engine. Applied Energy, 161: 320-329. https://doi.org/10.1016/j.apenergy.2015.10.042
[14] Masera, K., Hossain, A.K. (2019). Biofuels and thermal barrier: A review on compression ignition engine performance, combustion and exhaust gas emission. Journal of the Energy Institute, 92(3): 783-801. https://doi.org/10.1016/j.joei.2018.02.005
[15] Xu, L., Xu, S., Lu, X., Jia, M., Bai, X.S. (2023). Large eddy simulation of spray and combustion characteristics of biodiesel and biodiesel/butanol blend fuels in internal combustion engines. Applications in Energy and Combustion Science, 16: 100197. https://doi.org/10.1016/j.jaecs.2023.100197
[16] Jayed, M.H., Masjuki, H.H., Kalam, M.A., Mahlia, T.M. I., Husnawan, M., Liaquat, A.M. (2011). Prospects of dedicated biodiesel engine vehicles in Malaysia and Indonesia. Renewable and Sustainable Energy Reviews, 15(1): 220-235. https://doi.org/10.1016/j.rser.2010.09.002
[17] Kouzu, M., Hidaka, J. (2012). Transesterification of vegetable oil into biodiesel catalyzed by CaO: A review. Fuel, 93: 1-12. https://doi.org/10.1016/j.fuel.2011.09.015
[18] Kalargaris, I., Tian, G., Gu, S. (2016). Combustion, performance and emission analysis of a DI diesel engine using plastic pyrolysis oil. Fuel Processing Technology, 157: 108-115. https://doi.org/10.1016/j.fuproc.2016.11.016
[19] Shahid, E.M., Jamal, Y. (2011). Production of biodiesel: A technical review. Renewable and Sustainable Energy Reviews, 15(9): 4732-4745. https://doi.org/10.1016/j.rser.2011.07.079
[20] Viola, E., Blasi, A., Valerio, V., Guidi, I., Zimbardi, F., Braccio, G., Giordano, G. (2012). Biodiesel from fried vegetable oils via transesterification by heterogeneous catalysis. Catalysis Today, 179(1): 185-190. https://doi.org/10.1016/j.cattod.2011.08.050
[21] Knothe, G., Steidley, K.R. (2005). Kinematic viscosity of biodiesel fuel components and related compounds. Influence of compound structure and comparison to petrodiesel fuel components. Fuel, 84: 1059-1065. https://doi.org/10.1016/j.fuel.2005.01.016
[22] Klopfenstein, W.E. (1985). Effect of molecular weights of fatty acid esters on cetane numbers as diesel fuels. Journal of the American Oil Chemists' Society, 62(6): 1029-1031. https://doi.org/10.1007/BF02935708
[23] Ramírez-Verduzco, L.F., Rodríguez-Rodríguez, J.E., Jaramillo-Jacob, A. del R. (2012). Predicting cetane number, kinematic viscosity, density and higher heating value of biodiesel from its fatty acid methyl ester composition. Fuel, 91(1): 102-111. https://doi.org/10.1016/j.fuel.2011.06.070
[24] Mujtaba, M., Fernandes Fraceto, L., Fazeli, M., Mukherjee, S., Savassa, S.M., Araujo de Medeiros, G., do Espírito Santo Pereira, A., Mancini, S.D., Lipponen, J., Vilaplana, F. (2023). Lignocellulosic biomass from agricultural waste to the circular economy: A review with focus on biofuels, biocomposites and bioplastics. Journal of Cleaner Production, 402: 136815. https://doi.org/10.1016/j.jclepro.2023.136815

[25] Malode, S.J., Prabhu, K.K., Mascarenhas, R.J., Shetti, N.P., Aminabhavi, T.M. (2021). Recent advances and viability in biofuel production. Energy Conversion and Management: X, 10: 100070. https://doi.org/10.1016/j.ecmx.2020.100070
[26] Giakoumis, E.G. (2012). A statistical investigation of biodiesel effects on regulated exhaust emissions during transient cycles. Applied Energy, 98: 273-291. https://doi.org/10.1016/j.apenergy.2012.03.037
[27] Łagowski, P., Wcisło, G., Kurczyński, D. (2022). Comparison of the combustion process parameters in a diesel engine powered by second-generation biodiesel compared to the first-generation biodiesel. Energies, 15(18): 6835. https://doi.org/10.3390/en15186835
[28] Kumar, M.S., Kerihuel, A., Bellettre, J., Tazerout, M. (2006). Ethanol animal fat emulsions as a diesel engine fuel – Part 2: Engine test analysis. Fuel, 85(17-18): 2646-2652. https://doi.org/10.1016/j.fuel.2006.05.023
[29] Awad, S., Loubar, K., Tazerout, M. (2014). Experimental investigation on the combustion, performance and pollutant emissions of biodiesel from animal fat residues on a direct injection diesel engine. Energy, 69: 826-836. https://doi.org/10.1016/j.energy.2014.03.078
[30] Andreo-Martínez, P., Ortiz-Martínez, V.M., Salar-García, M.J., Veiga-del-Baño, J.M., Chica, A., Quesada-Medina, J. (2022). Waste animal fats as feedstock for biodiesel production using non-catalytic supercritical alcohol transesterification: A perspective by the PRISMA methodology. Energy for Sustainable Development, 69: 150-163. https://doi.org/10.1016/j.esd.2022.06.004
[31] Krieger, R.B., Borman, G.L. (1966). The computation of applied heat release for internal combustion engines, ASME. Paper 66-WA/DGP-4.
[32] Heywood, J.B., (1988). Internal Combustion Engines Fundamentals. Mc Graw Hill.